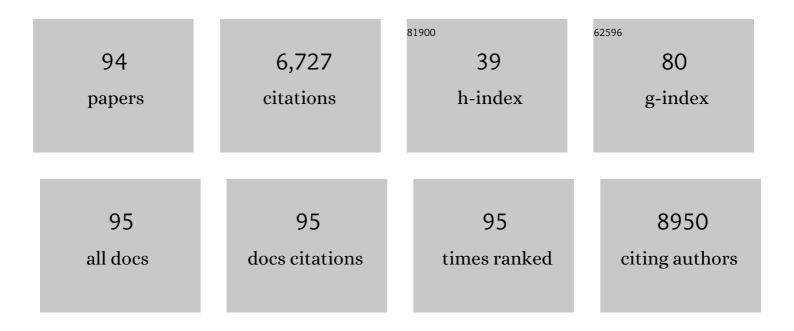
List of Publications by Year in descending order

Source: https://exaly.com/author-pdf/8138802/publications.pdf Version: 2024-02-01



BO SONG

#	Article	IF	CITATIONS
1	Contributions of Phase, Sulfur Vacancies, and Edges to the Hydrogen Evolution Reaction Catalytic Activity of Porous Molybdenum Disulfide Nanosheets. Journal of the American Chemical Society, 2016, 138, 7965-7972.	13.7	1,055
2	Efficient Electrocatalytic and Photoelectrochemical Hydrogen Generation Using MoS2 and Related Compounds. CheM, 2016, 1, 699-726.	11.7	462
3	Synergistic Phase and Disorder Engineering in 1Tâ€MoSe ₂ Nanosheets for Enhanced Hydrogenâ€Evolution Reaction. Advanced Materials, 2017, 29, 1700311.	21.0	411
4	2D Transition Metal Dichalcogenides: Design, Modulation, and Challenges in Electrocatalysis. Advanced Materials, 2021, 33, e1907818.	21.0	284
5	Tuning Mixed Nickel Iron Phosphosulfide Nanosheet Electrocatalysts for Enhanced Hydrogen and Oxygen Evolution. ACS Catalysis, 2017, 7, 8549-8557.	11.2	268
6	Modifying redox properties and local bonding of Co3O4 by CeO2 enhances oxygen evolution catalysis in acid. Nature Communications, 2021, 12, 3036.	12.8	262
7	Torsion strained iridium oxide for efficient acidic water oxidation in proton exchange membrane electrolyzers. Nature Nanotechnology, 2021, 16, 1371-1377.	31.5	197
8	S, N Dual-Doped Graphene-like Carbon Nanosheets as Efficient Oxygen Reduction Reaction Electrocatalysts. ACS Applied Materials & Amp; Interfaces, 2017, 9, 398-405.	8.0	194
9	Direct Transformation from Graphitic C ₃ N ₄ to Nitrogen-Doped Graphene: An Efficient Metal-Free Electrocatalyst for Oxygen Reduction Reaction. ACS Applied Materials & Interfaces, 2015, 7, 19626-19634.	8.0	182
10	Skutterudite-Type Ternary Co _{1–<i>x</i>} Ni _{<i>x</i>} P ₃ Nanoneedle Array Electrocatalysts for Enhanced Hydrogen and Oxygen Evolution. ACS Energy Letters, 2018, 3, 1744-1752.	17.4	160
11	Significantly Increased Raman Enhancement on MoX ₂ (X = S, Se) Monolayers upon Phase Transition. Advanced Functional Materials, 2017, 27, 1606694.	14.9	158
12	Highly Efficient Visible-Light-Driven Photocatalytic Hydrogen Production on CdS/Cu ₇ S ₄ /g-C ₃ N ₄ Ternary Heterostructures. ACS Applied Materials & Interfaces, 2018, 10, 20404-20411.	8.0	153
13	Defect-Induced Magnetism in Neutron Irradiated 6 <mml:math xmlns:mml="http://www.w3.org/1998/Math/MathML" display="inline"><mml:mi>H</mml:mi>-SiC Single Crystals. Physical Review Letters, 2011, 106, 087205.</mml:math 	7.8	143
14	MOFâ€Based Transparent Passivation Layer Modified ZnO Nanorod Arrays for Enhanced Photoâ€Electrochemical Water Splitting. Advanced Energy Materials, 2018, 8, 1800101.	19.5	143
15	Boosting Hydrogen Transfer during Volmer Reaction at Oxides/Metal Nanocomposites for Efficient Alkaline Hydrogen Evolution. ACS Energy Letters, 2019, 4, 3002-3010.	17.4	142
16	Stable and selective electrosynthesis of hydrogen peroxide and the electro-Fenton process on CoSe ₂ polymorph catalysts. Energy and Environmental Science, 2020, 13, 4189-4203.	30.8	134
17	Improving Electrocatalysts for Oxygen Evolution Using Ni _{<i>x</i>} Fe _{3–<i>x</i>} O ₄ /Ni Hybrid Nanostructures Formed by Solvothermal Synthesis. ACS Energy Letters, 2018, 3, 1698-1707.	17.4	132
18	Metal organic framework-derived CoPS/N-doped carbon for efficient electrocatalytic hydrogen evolution. Nanoscale, 2018, 10, 7291-7297.	5.6	107

#	Article	IF	CITATIONS
19	Observation of Glassy Ferromagnetism in Al-Doped 4H-SiC. Journal of the American Chemical Society, 2009, 131, 1376-1377.	13.7	103
20	Phaseâ€Junction Electrocatalysts towards Enhanced Hydrogen Evolution Reaction in Alkaline Media. Angewandte Chemie - International Edition, 2021, 60, 259-267.	13.8	91
21	The contribution of doped-Al to the colossal permittivity properties of Al _x Nb _{0.03} Ti _{0.97â^x} O ₂ rutile ceramics. Journal of Materials Chemistry C, 2016, 4, 6798-6805.	5.5	90
22	Bifunctional WC‣upported RuO ₂ Nanoparticles for Robust Water Splitting in Acidic Media. Angewandte Chemie - International Edition, 2022, 61, .	13.8	89
23	Unraveling the Raman Enhancement Mechanism on 1T′â€Phase ReS ₂ Nanosheets. Small, 2018, 14, e1704079.	10.0	87
24	Two-Dimensional High-Entropy Metal Phosphorus Trichalcogenides for Enhanced Hydrogen Evolution Reaction. ACS Nano, 2022, 16, 3593-3603.	14.6	77
25	Identification of the Active-Layer Structures for Acidic Oxygen Evolution from 9R-BalrO ₃ Electrocatalyst with Enhanced Iridium Mass Activity. Journal of the American Chemical Society, 2021, 143, 18001-18009.	13.7	73
26	Enhanced Electrocatalytic Oxygen Evolution Activity by Tuning Both the Oxygen Vacancy and Orbital Occupancy of Bâ€ s ite Metal Cation in NdNiO ₃ . Advanced Functional Materials, 2019, 29, 1902449.	14.9	72
27	Construction of FeP Hollow Nanoparticles Densely Encapsulated in Carbon Nanosheet Frameworks for Efficient and Durable Electrocatalytic Hydrogen Production. Advanced Science, 2019, 6, 1801490.	11.2	68
28	Facile synthesis of few-layer-thick carbon nitride nanosheets by liquid ammonia-assisted lithiation method and their photocatalytic redox properties. RSC Advances, 2014, 4, 32690-32697.	3.6	63
29	Ultrasmall MnO Nanoparticles Supported on Nitrogen-Doped Carbon Nanotubes as Efficient Anode Materials for Sodium Ion Batteries. ACS Applied Materials & Interfaces, 2017, 9, 38401-38408.	8.0	61
30	Magnetic field assisted electrocatalytic oxygen evolution reaction of nickel-based materials. Journal of Materials Chemistry A, 2022, 10, 1760-1767.	10.3	57
31	High-performance position-sensitive detector based on the lateral photoelectrical effect of two-dimensional materials. Light: Science and Applications, 2020, 9, 88.	16.6	53
32	Enhanced photocatalytic activity on polarized ferroelectric KNbO ₃ . RSC Advances, 2016, 6, 108883-108887.	3.6	50
33	Homogeneous Metal Nitrate Hydroxide Nanoarrays Grown on Nickel Foam for Efficient Electrocatalytic Oxygen Evolution. Small, 2018, 14, e1803783.	10.0	50
34	One-pot evaporation–condensation strategy for green synthesis of carbon nitride quantum dots: An efficient fluorescent probe for ion detection and bioimaging. Materials Chemistry and Physics, 2017, 194, 293-301.	4.0	47
35	Origin of the Ultrafast Response of the Lateral Photovoltaic Effect in Amorphous MoS ₂ /Si Junctions. ACS Applied Materials & Interfaces, 2017, 9, 18362-18368.	8.0	46
36	Metal-free nitrogen-doped carbon nanoribbons as highly efficient electrocatalysts for oxygen reduction reaction. Carbon, 2017, 124, 34-41.	10.3	46

#	Article	IF	CITATIONS
37	Ultrafine CoO nanoparticles as an efficient cocatalyst for enhanced photocatalytic hydrogen evolution. Nanoscale, 2019, 11, 15633-15640.	5.6	44
38	Sulfur vacancies promoting Fe-doped Ni ₃ S ₂ nanopyramid arrays as efficient bifunctional electrocatalysts for overall water splitting. Sustainable Energy and Fuels, 2020, 4, 3326-3333.	4.9	44
39	Large lateral photovoltaic effect with ultrafast relaxation time in SnSe/Si junction. Applied Physics Letters, 2016, 109, .	3.3	42
40	Synergistic modulation in MX ₂ (whereÂM = Mo or W or V, and X = S or Se) for an enhanced hydrogen evolution reaction. Journal of Materials Chemistry A, 2018, 6, 21847-21858.	10.3	39
41	Mixed Titanium Oxide Strategy for Enhanced Photocatalytic Hydrogen Evolution. ACS Applied Materials & Interfaces, 2019, 11, 18475-18482.	8.0	39
42	Controlled Synthesis of Hollow Bimetallic Prussian Blue Analog for Conversion into Efficient Oxygen Evolution Electrocatalyst. ACS Sustainable Chemistry and Engineering, 2020, 8, 1319-1328.	6.7	39
43	Magnetic Field Enhanced Electrocatalytic Oxygen Evolution of NiFeâ€LDH/Co ₃ O ₄ pâ€n Heterojunction Supported on Nickel Foam. Small Methods, 2022, 6, e2200084.	8.6	39
44	Anion-Induced Size Selection of β-Mo ₂ C Supported on Nitrogen-Doped Carbon Nanotubes for Electrocatalytic Hydrogen Evolution. ACS Sustainable Chemistry and Engineering, 2018, 6, 11922-11929.	6.7	38
45	Experimental observation of defect-induced intrinsic ferromagnetism in III-V nitrides: The case of BN. Physical Review B, 2009, 80, .	3.2	35
46	A confined "microreactor―synthesis strategy to three dimensional nitrogen-doped graphene for high-performance sodium ion battery anodes. Journal of Power Sources, 2018, 378, 105-111.	7.8	34
47	Observation of the Long Afterglow in AlN Helices. Nano Letters, 2015, 15, 6575-6581.	9.1	33
48	Two Are Better than One: Heterostructures Improve Hydrogen Evolution Catalysis. Joule, 2017, 1, 220-221.	24.0	32
49	Phase-junction engineering boosts the performance of CoSe ₂ for efficient sodium/potassium storage. Journal of Materials Chemistry A, 2021, 9, 25954-25963.	10.3	30
50	Near-ultraviolet lateral photovoltaic effect in Fe_3O_4/3C-SiC Schottky junctions. Optics Express, 2016, 24, 23755.	3.4	27
51	Dualâ€Enhanced Doping in ReSe ₂ for Efficiently Photoenhanced Hydrogen Evolution Reaction. Advanced Science, 2020, 7, 2000216.	11.2	26
52	Phaseâ€Junction Electrocatalysts towards Enhanced Hydrogen Evolution Reaction in Alkaline Media. Angewandte Chemie, 2021, 133, 263-271.	2.0	24
53	Ruthenium Incorporated Cobalt Phosphide Nanocubes Derived From a Prussian Blue Analog for Enhanced Hydrogen Evolution. Frontiers in Chemistry, 2018, 6, 521.	3.6	23
54	Self-powered ultraviolet vertical and lateral photovoltaic effect with fast-relaxation time in NdNiO3/Nb:SrTiO3 heterojunctions. Applied Physics Letters, 2018, 112, .	3.3	22

#	Article	IF	CITATIONS
55	Single-crystalline melem (C ₆ N ₁₀ H ₆) nanorods: a novel stable molecular crystal photocatalyst with modulated charge potentials and dynamics. Journal of Materials Chemistry A, 2019, 7, 13234-13241.	10.3	22
56	Investigating the electroactivity of nitrogen species in MoC nanoparticles/N-doped carbon nanosheets for high-performance Na/Li-ion batteries. Journal of Materials Chemistry A, 2020, 8, 21298-21305.	10.3	22
57	Beyond 1Tâ€phase? Synergistic Electronic Structure and Defects Engineering in 2Hâ€MoS _{2x} Se _{2(1â€x)} Nanosheets for Enhanced Hydrogen Evolution Reaction and Sodium Storage. ChemCatChem, 2019, 11, 3200-3211.	3.7	21
58	The sublimation growth of AlN fibers: transformations inÂmorphology & fiber direction. Applied Physics A: Materials Science and Processing, 2009, 94, 173-177.	2.3	20
59	Magnetoresistance reversal in antiperovskite compound Mn3Cu0.5Zn0.5N. Journal of Applied Physics, 2014, 115, 123905.	2.5	19
60	Helical Growth of Aluminum Nitride: New Insights into Its Growth Habit from Nanostructures to Single Crystals. Scientific Reports, 2015, 5, 10087.	3.3	18
61	Bifunctional Ag/C ₃ N _{4.5} composite nanobelts for photocatalysis and antibacterium. Nanotechnology, 2016, 27, 395603.	2.6	16
62	Experimental observation of ferromagnetism evolution in nanostructured semiconductor InN. Journal of Materials Chemistry, 2010, 20, 9935.	6.7	15
63	Quantum dot-induced improved performance of cadmium telluride (CdTe) solar cells without a Cu buffer layer. Journal of Materials Chemistry A, 2017, 5, 4904-4911.	10.3	14
64	Na0.9Ni0.45Ti0.55O2 as novel bipolar material for sodium ion batteries. Solid State Ionics, 2019, 334, 14-20.	2.7	14
65	Bifunctional WCâ€Supported RuO ₂ Nanoparticles for Robust Water Splitting in Acidic Media. Angewandte Chemie, 2022, 134, .	2.0	11
66	Temperature dependence of the A1(LO) and E2 (high) phonons in hexagonal InN nanowires. Journal of Applied Physics, 2007, 101, 124302.	2.5	9
67	Magnetic mechanism investigations on n-type ferromagnetic Li(Zn,Mn)As. Solid State Communications, 2014, 177, 113-116.	1.9	9
68	Fabrication of Hâ€īiO ₂ /CdS/Cu _{2â€<i>x</i>} S Ternary Heterostructures for Enhanced Photocatalytic Hydrogen Production. ChemistrySelect, 2017, 2, 2681-2686.	1.5	9
69	Bulk GaN single crystals: a reinvestigation of growth mechanism using Li3N flux. Applied Physics A: Materials Science and Processing, 2006, 85, 169-172.	2.3	8
70	Effect of Oxygen-deficiencies on Resistance Switching in Amorphous YFe0.5Cr0.5O3â^'d films. Scientific Reports, 2016, 6, 30335.	3.3	8
71	Defect Engineering in Metastable Phases of Transitionâ€Metal Dichalcogenides for Electrochemical Applications. Chemistry - an Asian Journal, 2020, 15, 3961-3972.	3.3	8
72	MOFâ€derived Multiâ€Shelled NiP ₂ Microspheres as Highâ€Performance Anode Materials for Sodium″Potassium″on Batteries. Advanced Energy and Sustainability Research, 2022, 3, .	5.8	7

#	Article	IF	CITATIONS
73	Growth of GaN Single Crystals by Li ₃ N Flux with Mn as Addition. Crystal Growth and Design, 2008, 8, 2775-2779.	3.0	6
74	New diluted magnetic semiconductor (BaK)(ZnMn)2As2: Electronic structure and magnetic properties. Computational Materials Science, 2015, 98, 93-98.	3.0	6
75	Vacancy defect complexes in silicon: Charges and spin order. Physical Review B, 2016, 94, .	3.2	6
76	Transition from antiferromagnetic ground state to robust ferrimagnetic order with Curie temperatures above 420 K in manganese-based antiperovskite-type structures. Journal of Materials Chemistry C, 2018, 6, 13336-13344.	5.5	5
77	Mn-N-P doped carbon spheres as an efficient oxygen reduction catalyst for high performance Zn-Air batteries. Chinese Chemical Letters, 2023, 34, 107222.	9.0	5
78	Effects of Transition Metal (TM = V, Cr, Mn, Fe, Co, and Ni) Elements on Magnetic Mechanism of LiZnP with Decoupled Charge and Spin Doping. Journal of Superconductivity and Novel Magnetism, 2017, 30, 2823-2828.	1.8	4
79	First-principles study on electronic and magnetic properties of (Al,Mn) codoped BaZn2As2. Journal of Alloys and Compounds, 2019, 783, 387-392.	5.5	4
80	Siteâ€Selective Chlorination of Graphene through Laserâ€Induced In Situ Decomposition of AgCl Nanoparticles, ChemNanoMat, 2016, 2, 515-519.	2.8	3
81	<mml:math <br="" display="inline" xmlns:mml="http://www.w3.org/1998/Math/Math/MathML">overflow="scroll"><mml:mrow><mml:mi>Al</mml:mi><mml:mi mathvariant="normal">N</mml:mi </mml:mrow></mml:math> Nanowires and <mml:math xmlns:mml="http://www.w3.org/1998/Math/MathML" display="inline"</mml:math 	3.8	3
82	Phase engineering of transition metal compounds for boosting lithium/sodium storage. APL Materials, 2021, 9, .	5.1	3
83	First principles study on ferromagnetism of diluted magnetic semiconductor Li(Zn, Mn)N. Journal of Applied Physics, 2018, 124, 203901.	2.5	2
84	Investigations on ferromagnetism of Li and Mn codoped LiZnN by firstâ€principles calculations. Journal of the American Ceramic Society, 2019, 102, 303-309.	3.8	2
85	Electronic structure of multiferroic BiFeO3: Electron energy-loss spectroscopy and first-principles study. Micron, 2019, 120, 43-47.	2.2	2
86	Highly Active Sites in Quaternary LnPdAsO (Ln = La, Ce, Pr) with Excellent Catalytic Activity for Hydrogen Evolution Reaction. ACS Applied Energy Materials, 2021, 4, 4302-4307.	5.1	2
87	Interface regulation promoting carbon monoxide gas diffusion electrolysis towards C _{2⁺} products. Chemical Communications, 2022, 58, 3645-3648.	4.1	2
88	Significantly enhanced mechanical properties in AlN helix. Nanotechnology, 2017, 28, 275703.	2.6	1
89	Heating- and magnetization-stimulated increase in the Néel temperature and saturation field of iron-enriched garnet films. Journal of Magnetism and Magnetic Materials, 2022, 552, 169215.	2.3	1
90	Investigations on electronic structure of YMnO3 by electron energy loss spectra and first-principle calculations. Powder Diffraction, 2019, 34, 339-344.	0.2	0

#	Article	IF	CITATIONS
91	Investigations on p- and n-type diluted magnetic semiconductors X/Mn-codoped LiZnN (X= Li, Na and K). Journal of Alloys and Compounds, 2020, 821, 153235.	5.5	0
92	3D-Ising critical behavior in antiperovskite-type ferromagneticlike Mn3GaN. Journal of Applied Physics, 2020, 127, 073903.	2.5	0
93	Frontispiece: Phaseâ€Junction Electrocatalysts towards Enhanced Hydrogen Evolution Reaction in Alkaline Media. Angewandte Chemie - International Edition, 2021, 60, .	13.8	0
94	Frontispiz: Phaseâ€Junction Electrocatalysts towards Enhanced Hydrogen Evolution Reaction in Alkaline Media. Angewandte Chemie, 2021, 133, .	2.0	0